Jpn. J. Appl. Phys. Vol. 40 (2001) pp. 824–831
Part 1, No. 2A, February 2001

Analysis of Exploding Plasma Behavior in a Dipole Magnetic Field

Takanobu MURANAKA*, Hideyuki UCHIMURA, Hideki NAKASHIMA, Yuri P. ZAKHAROV[1], Sergey A. NIKITIN[2] and Arnold G. PONOMARENKO[1]

Department of Advanced Energy Engineering Science, Kyushu University, 6-1 Kasuga-Kouen, Kasuga, Fukuoka 816-8580, Japan
[1]*Institute of Laser Physics, Novosibirsk 630090, Russia*
[2]*Budker Institute of Nuclear Physics, Novosibirsk 630090, Russia*

(Received June 30, 2000; accepted for publication October 17, 2000)

Numerical analyses on plasma behaviors in a dipole magnetic field are performed using a three-dimensional (3D) hybrid code. Results are compared with the experimental data and magnetohydrodynamics (MHD) analysis. Dependence of plasma expansion on initial plasma energy and location are discussed by temporal evolutions of plasma position and magnetic field strength. An overall good agreement in the expansion behavior of plasmas among these results is found. The asymmetrical shape of the expanding plasma in the cross-field direction is also noticed, and the reason for this is discussed. For future engineering applications, these results will be useful in designing an optimal configuration of the magnetic thrust chamber for laser fusion rockets, and for studying the effective explosive methods for protecting the earth from collisions by asteroids or comets.

KEYWORDS: laser produced plasma, dipole magnetic field, three-dimensional hybrid code, interaction parameter

1. Introduction

Many basic studies on laser produced plasma under an ambient magnetic field have been performed for the purpose of future applications such as in direct energy conversion from fusion reactors. High-energy plasmas expand into a vacuum space with interactions with the ambient external magnetic fields. From the viewpoint of controlling plasma expansion to protect a chamber wall of the reactor, it is necessary to determine the configuration and location of its expanding surface and to determine its propagation limit. Because of the nonlinear nature of the interacting process, numerical analysis has been a useful aid to study these complex physics reactions.

In the fields of astrophysics, Nikitin and Ponomarenko[1)] have analyzed the dynamics of three-dimensional (3D) plasma expansion for a dipole field configuration in the framework of the ideal magnetohydrodynamics (MHD) approximation. Their interests lie in nonstationary processes of an explosive nature in cosmic plasma, and in particular, in the global instability of the earth's magnetosphere for estimating the effective explosive methods for protecting it from collisions by asteroids or comets.[2)] Their model was compared with the results of an experiment on the expansion of the laser produced plasma cloud. They have found an important parameter (κ) characterizing the interaction of the expanding plasma cloud with the dipole field.[1)]

We have numerically studied the behaviors of expanding plasma under various magnetic fields.[3–5)] Analyses were carried out on magnetic field modeling a magnetic thrust chamber for a laser fusion rocket using a 3D hybrid code.[4,5)] The hybrid code treats ions as individual particles and electrons as a fluid. The magnetic field adopted there was produced by a single solenoidal coil and hence the magnetic field structure was a variant from a dipole type field, since decreasing coil radius could reproduce the dipole field configuration. The interaction between plasma and a properly designed magnetic field could convert initial isotropic kinetic motion of plasma to directed motion for thrust generation. Nikitin and Ponomarenko have applied the same MHD method to estimate the thrust efficiency in the magnetic thrust chamber and compared their results to those from the 3D hybrid code.[6)] They have found a good agreement between them.

The MHD approximation is a very useful approach to examine global motion of high-density magnetized plasma. However, it would not be suitable for analysis of a system where the particle motion of plasma is dominant. In addition, it is not that easy to follow a complex surface or boundary with the numerical MHD simulation. In the dipole field, the spatial distribution of magnetic field strength varies considerably, so an ion's finite Larmor motion should not be neglected locally. Moreover, it is considered that the plasma cloud surface forms a very complex shape. Thus applying a hybrid code for the analysis of an ion's motion in the dipole field seems reasonable.

In this paper, we study plasma behaviors in a dipole magnetic field using the 3D hybrid code. In §2, the numerical model adopted here is introduced. The experimental setup and its characteristic parameters are briefly mentioned in §3. Section 4 presents comparison of results from the 3D hybrid code with the experimental data and the MHD analysis. Dependences of the expansion behaviors on initial plasma energy and location are also discussed. Finally, the conclusions are given in §5.

2. Numerical Model

To calculate the plasma behavior under the dipole magnetic field, we have developed a 3D hybrid particle-in-cell (PIC) code based on the model given in ref. 7. The hybrid code treats ions as individual particles and electrons as a fluid. This approach is valid when the system behavior is dominated by ion physics. The motion of an ion is solved self-consistently, that is, ions affect magnetic and electric fields, and ions are moved under the fields.

The basic equations of the model are as follows.

The electric field is computed from the momentum equation for an electron fluid

$$n_e m_e (dv_e/dt) = -en_e(E + v_e \times B) - \nabla P_e, \qquad (1)$$

*Corresponding author. E-mail: taka@aees.kyushu-u.ac.jp

where m_e is the electron mass, n_e the electron density, e the elementary electric charge, $\boldsymbol{v}_e$ the electron velocity, $\boldsymbol{E}$ the electric field, and $\boldsymbol{B}$ the total magnetic field. P_e is the electron pressure given by

$$P_e = n_e T_e, \tag{2}$$

where T_e is the electron temperature and it is assumed to be uniform for the sake of simplicity.

The electrons are approximated as a massless fluid, so the left-hand side of eq. (1) becomes zero, and

$$\boldsymbol{E} = -\boldsymbol{v}_e \times \boldsymbol{B} - (1/en_e)\nabla P_e. \tag{3}$$

Ampere's Law with Darwin approximation, which means that high-frequency electromagnetic waves do not exist, reduces to

$$\nabla \times \boldsymbol{B}_p = \mu_0(\boldsymbol{J}_e + \boldsymbol{J}_i). \tag{4}$$

where $\boldsymbol{B}_p$ is the magnetic field generated by the plasma current density. Substituting $-en_e\boldsymbol{v}_e$ for $\boldsymbol{J}_e$ in Ampere's law, solving for $\boldsymbol{v}_e$, and substituting $\boldsymbol{v}_e$ into eq. (3), we obtain

$$\begin{aligned}\boldsymbol{E} = {} & (1/\mu_0 Zen_i)(\nabla \times \boldsymbol{B}_p) \times \boldsymbol{B} \\ & - (1/Zen_i)\boldsymbol{J}_i \times \boldsymbol{B} - (T_e/en_i)\nabla n_i.\end{aligned} \tag{5}$$

We assume quasi-neutrality and set the ion charge density equal to the electron charge density, i.e.,

$$Zn_i = n_e \tag{6}$$

in eq. (5), where Z is the charge state of the ion. Equation (5) includes the terms inversely proportional to the ion's number density n_i. In a vacuum region, these terms must cause numerical infinity. We solve the Laplace equation to obtain the electric field in the vacuum region,

$$\nabla^2 \boldsymbol{E} = 0. \tag{7}$$

The ion density n_i and the current density $\boldsymbol{J}_i$ are calculated by the PIC method from particle position $\boldsymbol{x}_i$ and velocity $\boldsymbol{v}_i$ which are obtained by integrating the equations of motion. The equations are given as follows

$$d\boldsymbol{v}_i/dt = (Ze/m_i)(\boldsymbol{E} + \boldsymbol{v}_i \times \boldsymbol{B}), \tag{8}$$

$$d\boldsymbol{x}_i/dt = \boldsymbol{v}_i, \tag{9}$$

where m_i is the mass, Ze the charge, $\boldsymbol{v}_i$ the velocity, and $\boldsymbol{x}_i$ the position of the ion.

The magnetic field is advanced by Faraday's law

$$\partial \boldsymbol{B}/\partial t = -\nabla \times \boldsymbol{E}. \tag{10}$$

Cartesian coordinates ($X \times Y \times Z$) are adopted here. The time levels of the ion's position and field quantities are defined at an integer time step, and the ion's velocity and the current density at half time step. The leap-frog method which is a time centered difference scheme is adopted to solve the ion's equation of motion. Faraday's law is solved with the backward difference scheme in time. Field quantities, number density and current density are spatially defined at the same grid points. The boundary condition adopted here for the field quantities is that the spatial differences of the normal components are set to be zero at the surface of the cylindrical calculation region.

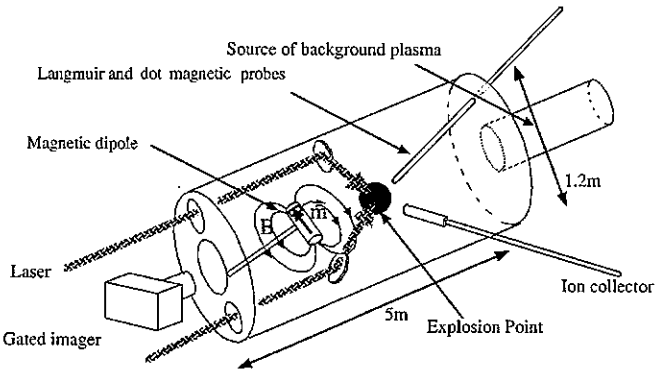

Fig. 1. Schematic of experimental facility.

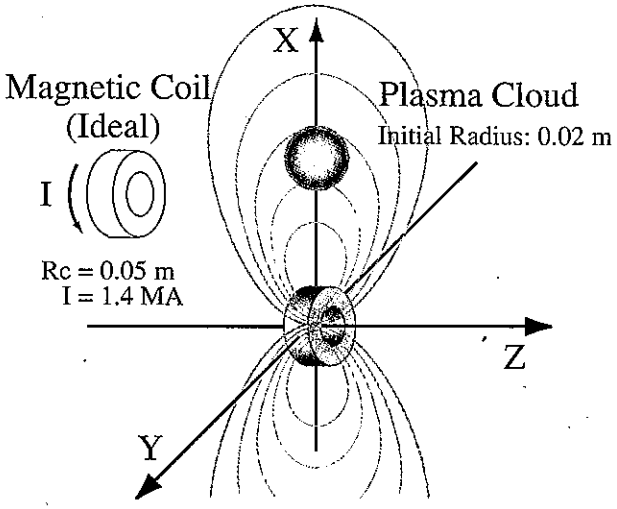

Fig. 2. Schematic of the calculation model.

Table I. Experimental parameters.

Distance of dipole center to the target R_0 (cm)	22
Dipole magnetic moment $\|m\|$ (MG · cm^3)	11
Initial magnetic field at $R = R_0$ (T)	0.11
Initial kinetic energy E_0 (J)	8 ($\kappa = 0.02$)
	13 ($\kappa = 0.036$)
Ion charge state Z (H^+ 50%, C^{4+} 50%)	2.5
Ion mass (AMU)	6.5

3. Experiments

For the comparative analysis, we will use the data of an experiment in ref. 1 where a quasi-spherical plasma cloud was produced by means of the bilateral symmetric action of a CO_2 laser pulse on a small Nylon 6 $(C_6H_{11}ON)_n$ target. Figure 1 shows the schematic of the experimental setup. The target was placed in a vacuum chamber near a current coil with magnetic moment magnitude $|\boldsymbol{m}| = 11\,\mathrm{MG{\cdot}cm^3}$. The experimental parameters are given in Table I. H^+ and C^{4+} ions were mainly generated under these conditions. We assumed a single kind of plasma with charge state Z of +2.5 and mass of 6.5 amu by taking the average quantities of these two kinds of ions. This is because we focused here on a numerical simulation for analyzing the macroscopic plasma behavior. (We also performed the same calculation for a single C^{4+} ion and found almost the same macroscopic behaviors mentioned below.)

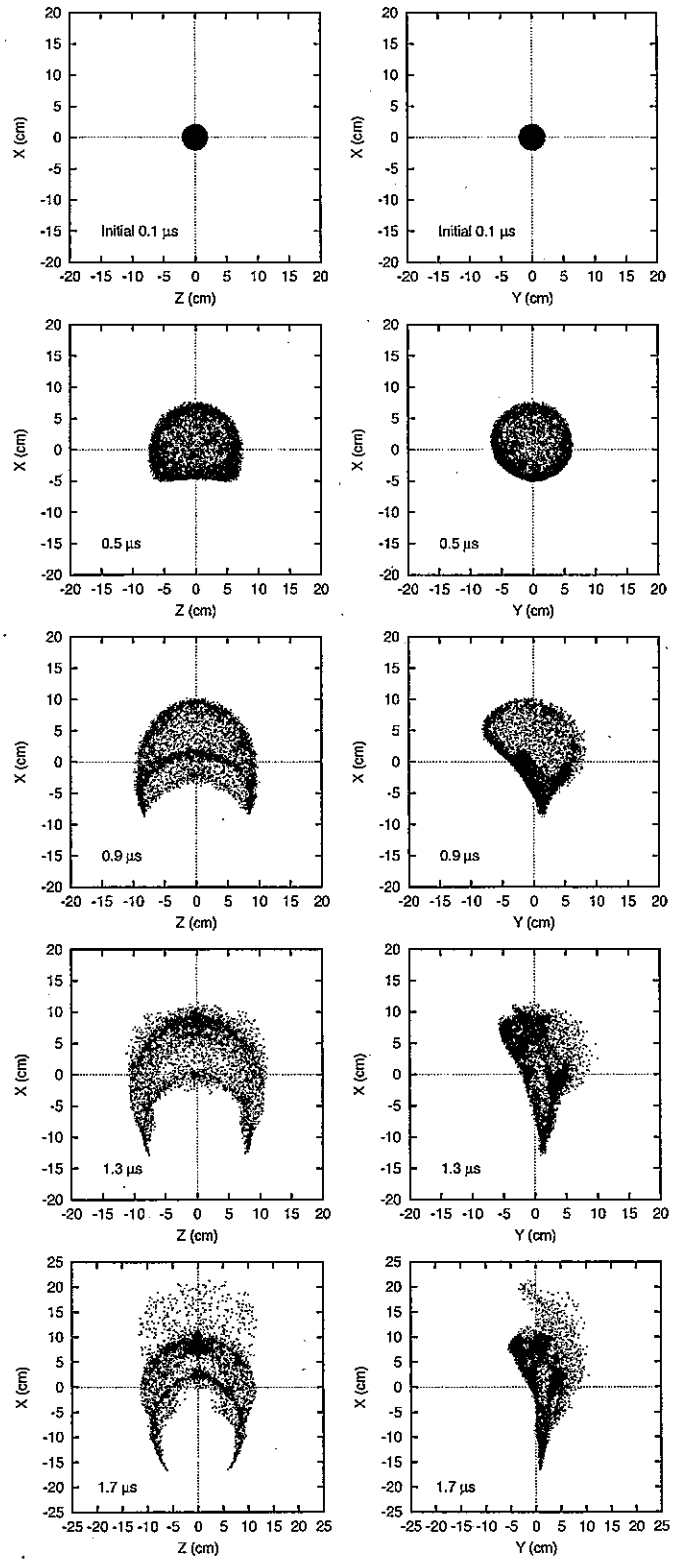

Fig. 3. Simulation results of particle positions projected onto (a) xz plane (left) and (b) xy plane (right) ($\kappa = 0.02$).

Nikitin defined a parameter (interaction parameter) κ which characterizes the interaction between the expanding plasma and the dipole field[1)] and is given as

$$\kappa = \frac{E_0}{E_M} = \frac{3E_0R_0^3}{|m|^2}, \tag{11}$$

where E_0 is the initial kinetic energy of an ion and E_M the field energy integral of the dipole within a spherical radius R_0 ($E_M = |m|^2/3R_0^3$). The parameter has a critical value of 0.1. In the case where κ is lower than 0.1, a substantial plasma deceleration will occur in all directions from the explosion location ("quasi-capture" mode), meanwhile the plasma will not be captured by an ambient field when κ is greater than 0.1 ("rupture" mode).

First, the explosion is assumed to take place in the equatorial plane at radius $R_0 = 22$ cm at a point with field strength $B = 0.11$ T. The kinetic energy of the plasma cloud E_0 is 8 or 13 J. The interaction parameters are estimated from Table I to be 0.02 and 0.036 when the initial kinetic energies are 8 J and 13 J, respectively, corresponding to "quasi-capture" mode.

Next, another initial plasma position different from that in the above mentioned experiments is also assumed. Details are explained in a later section.

4. Comparison with Experimental Data and MHD Analysis

In this section, we will present three kinds of simulation results along with the experimental results and the MHD analyses. First, two "quasi-capture" mode simulations are presented for the cases where the locations of the initial plasma are different (§4.1 and 4.2). Next, a "rupture" mode simulation is presented (§4.3). Discussions and comparisons are also made among these results.

4.1 "Quasi-capture" mode analysis

The plasma behaviors were calculated by the 3D hybrid code under the plasma conditions of "quasi-capture" mode. Initial plasma was located on the x-axis at radius R_0 as shown in Fig. 2. It was assumed to have a radius of 2 cm with a mass of 1 μg and its maximum velocity V_m was 170 km/s with initial plasma energy of 8 J ($\kappa = 0.02$). Initial distributions of the particle positions and velocities were assumed to be uniform. The dimensions ($X \times Y \times Z$) of the calculation region are 90 cm $\times$ 90 cm $\times$ 90 cm, and the center is the initial position of the plasma. The mesh size adopted is $(1.5\,\text{cm})^3$. The number of simulated particles is 100,000 which are assumed to be a single kind of ion with charge state 2.5 and mass 6.5 by taking average quantities of 50% of H^+ and 50% of C^{4+}. The coil to produce the dipole field is assumed to have a radius of 5 cm with a current density of 1.4 MA to generate the same field strength of 0.11 T at the initial plasma point R_0 similar to the experiment.

Numerical results for the time evolutions of particle positions are shown in Figs. 3(a) and 3(b), where they are projected onto the xz and xy planes, respectively. Here, the simulation starts from $t = 0.1$ μs to take account of the time elapsed for the plasma expansion to 2 cm in radius. As seen in Fig. 3(a), the plasma shape is spherical at the initial stage and the plasma expands almost isotropically, and then some downward ions are reflected by the external magnetic field, and its shape changes to follow the dipole magnetic field line. It is found that the main body of plasma particles was captured by the dipole magnetic field in the xz plane.

On the other hand, as shown in Fig. 3(b) an initially symmetrical plasma cloud begins to be asymmetric in the xy plane (cross field plane) after 0.5 μs. Figures 4(a) and 4(b) show the time evolution of velocity distribution projected onto the xz and xy planes at an early stage. Figures 5 shows plots of ion

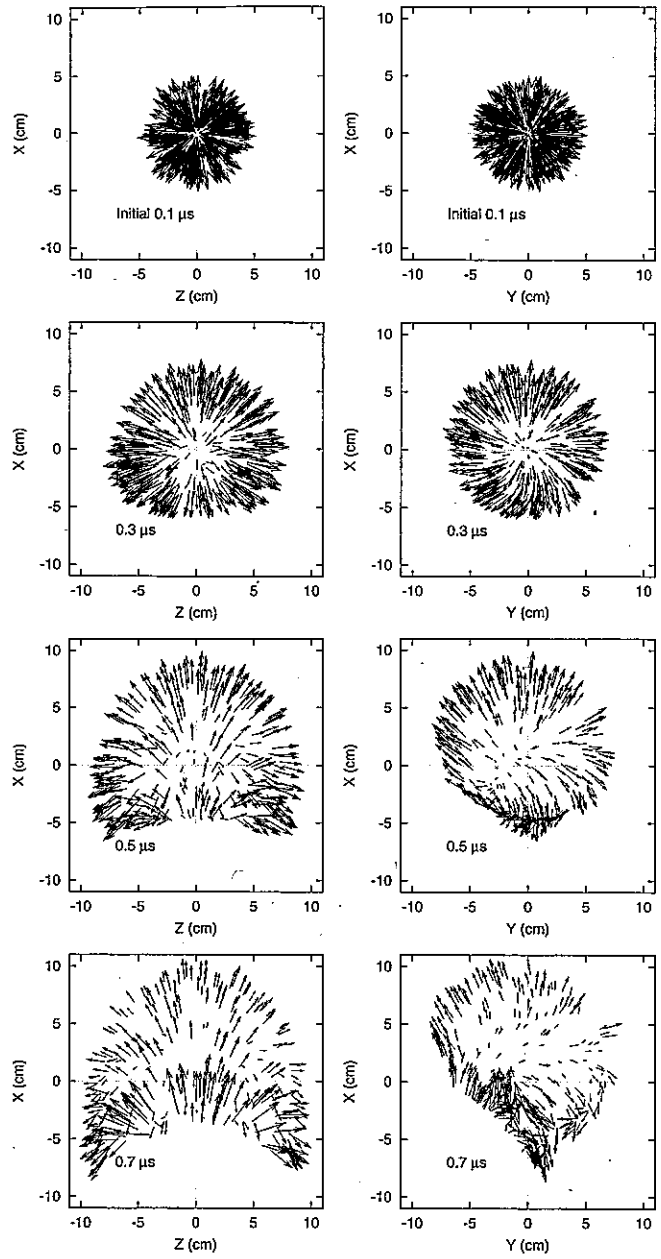

Fig. 4. Time evolution of velocity distribution at an early stage projected onto the (a) xz plane (left), and (b) xy plane (right) ($\kappa = 0.02$). The maximum velocity V_m is 170 km/s.

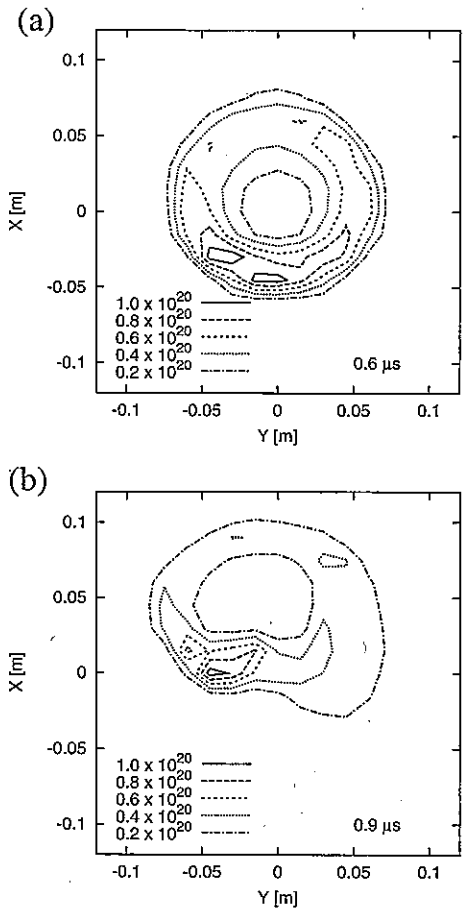

Fig. 5. Numerical results of ion number density contour on xy plane at $z = 0$ at time (a) $t = 0.6$ and (b) $t = 0.9\,\mu$s after laser pulse ($\kappa = 0.02$).

number density contours on the xy plane at $z = 0$ at two different times. From these figures, this asymmetrical pattern is thought to be caused by the following reasons which are briefly illustrated in Fig. 6.

At the initial stage, the plasma cloud expands isotropically as a free stream with high kinetic energy [Fig. 6(a)]. Then, plasma expanding downward begins to decelerate because the ambient field is stronger at a lower region near the coil [Fig. 6(b)]. Kinetic beta β_k defined as the ratio of plasma kinetic energy density to magnetic energy density reaches unity around this area first, and then strong interaction between plasma and the ambient field occurs. Thus, the diamagnetic motion of plasma is induced to generate the surface diamagnetic current asymmetrically, only on the lower plasma surface [Fig. 6(c)]. The asymmetrical diamagnetic motion of plasma generates the divergence of plasma from the right side of the cloud, while the plasma is concentrated around the left side [Fig. 6(d)]. The densification around the left side of the cloud is also shown in Fig. 5. In the end, on the right surface of the plasma cloud, the force inducing its diamagnetic motion could balance against the external magnetic field pressure which causes bounce motion of the plasma. On the left side of the surface, the bounce motion of plasmas occurs because of the absence of the force against the external field pressure. That makes the shape of the cloud asymmetrical.

Figure 7(a) shows a picture taken at time $= 1.73\,\mu$s after the laser pulse for the case of $\kappa = 0.02$ with the initial plasma energy of 8 J on the xz plane and Fig. 7(b) shows that on the xy plane. We found from these results that the plasma particles were still captured by the dipole magnetic field and the asymmetry of the plasma cloud on the xy plane similar to the numerical results was observed.

Figure 8(a) shows numerical results for the case of $\kappa = 0.02$ of the time evolution of magnetic field strength on the x-axis and (b) spatial distribution of the magnetic field on the xy plane at $z = 0$ at $t = 0.6\,\mu$s. Plasma expands by compressing the external field at the early stage [Fig. 8(a)] and the diamagnetic cavity is formed [Figs. 8(a) and 8(b)].

Figure 9(a) shows the front of the plasma cloud obtained with the aid of a sensitive image-converter tube at time $t = 0.7\,\mu$s after the laser pulse in the case of initial plasma energy 13 J ($\kappa = 0.036$). Also shown here for comparison are the results from the MHD calculations indicated by the shaded area. Figure 9(b) shows a plot of particle positions obtained

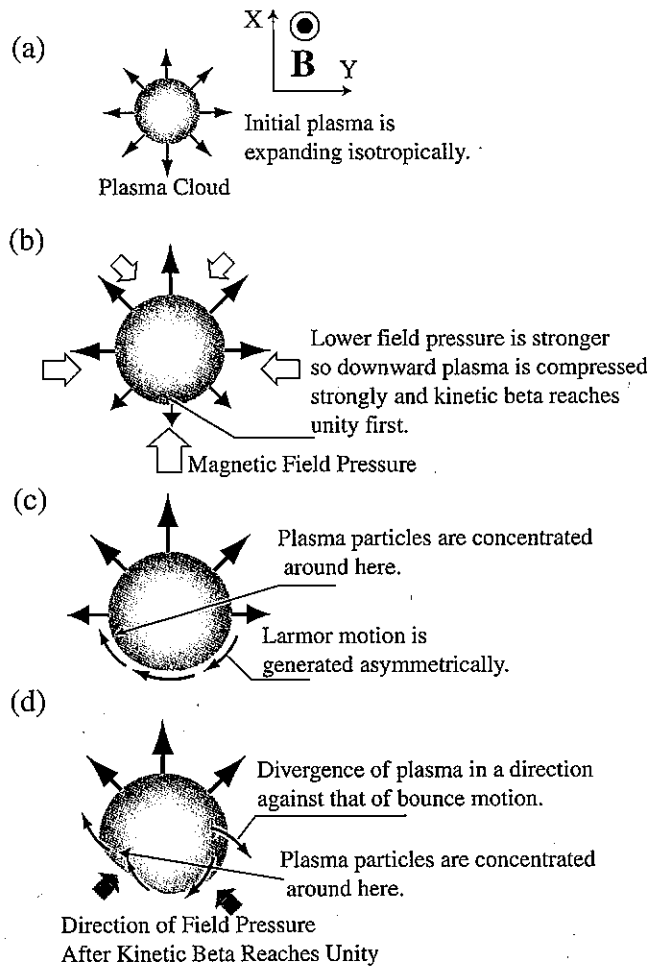

Fig. 6. Schematics explaining a macroscopic asymmetrical shape of plasma cloud.

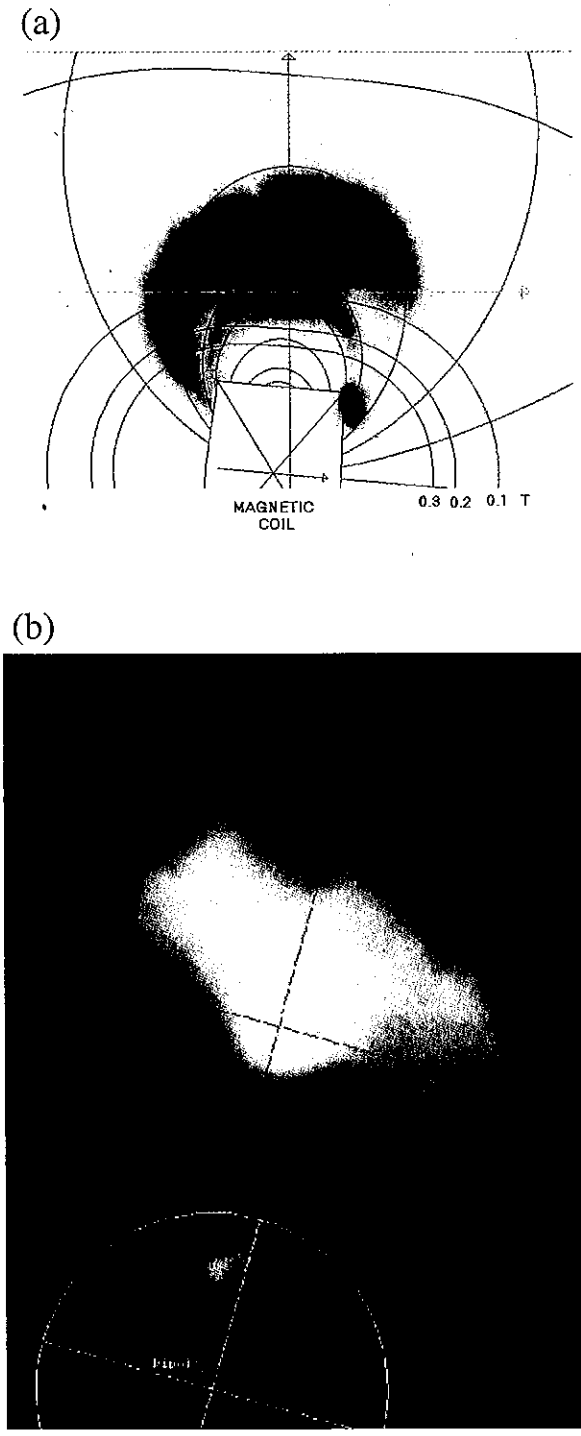

Fig. 7. Experimental data of plasma cloud at time $t = 1.7\,\mu$s after laser pulse (a) view on xz plane and (b) on xy plane ($\kappa = 0.02$).

from the 3D hybrid calculation. The maximum velocity of the plasma, V_m was 228 km/s. From these results, we found an overall good agreement among the MHD analysis, the experimental result and numerical results. A densification of the particles is observed in the plot of the simulation results [Fig. 9(b)], due to the reflection of particles from the inner magnetic field.

Comparison among our numerical results by the 3D hybrid code, the MHD analysis and the experimental results, showed overall good agreement with regard to the motion of plasma cloud and its macroscopic shape. The plasma cloud was captured in the dipole field under these experimental conditions and it followed the magnetic field line. Finally, the plasma cloud had an asymmetrical shape in the cross-field direction, which could not be predicted by the MHD analysis.

4.2 *Angular dependence of plasma explosion*

In this section, we have analyzed the plasma motion with its initial location being 30° from the z-axis as shown in Fig. 10. Other parameters are the same as mentioned in §4.1, and the plasma explosion point is located at the distance $R_0 = 0.22$ m from the dipole center. The field strength has the same value of 0.11 T.

Figure 11 shows the experimental results observed by an image camera at $t = 0.55\,\mu$s after laser irradiation. Figure 12 shows the time evolution of plasma positions projected onto the xz-plane as calculated by the hybrid code. It is found that the plasma cloud expands under the influence of the ambient field and its center moves apart at an almost constant speed. The movement speed calculated by these results is about 100 km/s. Note that during 1.1 to 1.4 μs an abrupt explosion occurred around the point $(x, y) = (7, 7\,\text{cm})$. In this case, the plasma cloud was not captured even when the parameter κ was much less than unity. This result is also in good agreement with the experimental one.

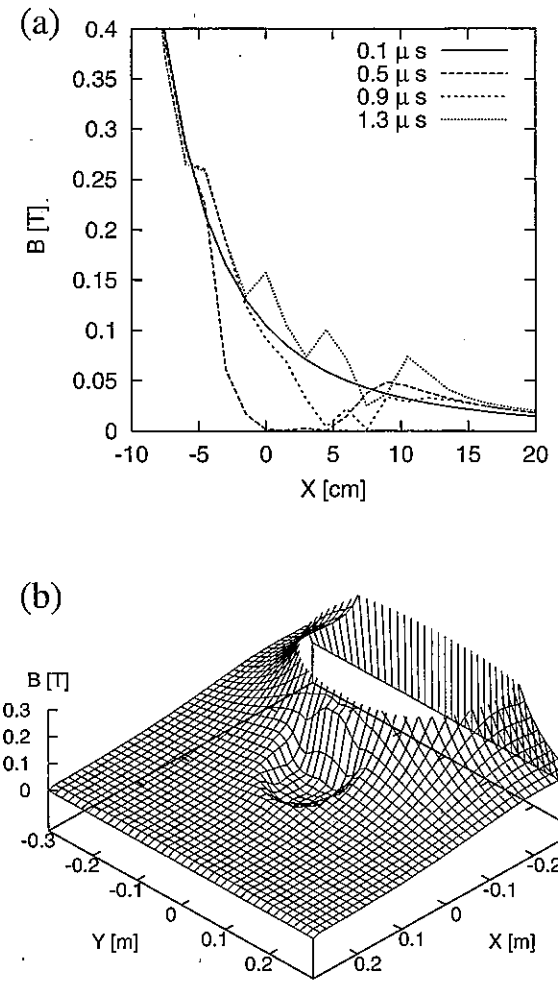

Fig. 8. Numerical results of (a) time evolution of magnetic field strength on x-axis and (b) spatial distribution of magnetic field strength on xy plane at z=0 at $t = 0.6\,\mu$s ($\kappa = 0.02$). The values of X and Y axes indicate the distance from the initial plasma explosion point.

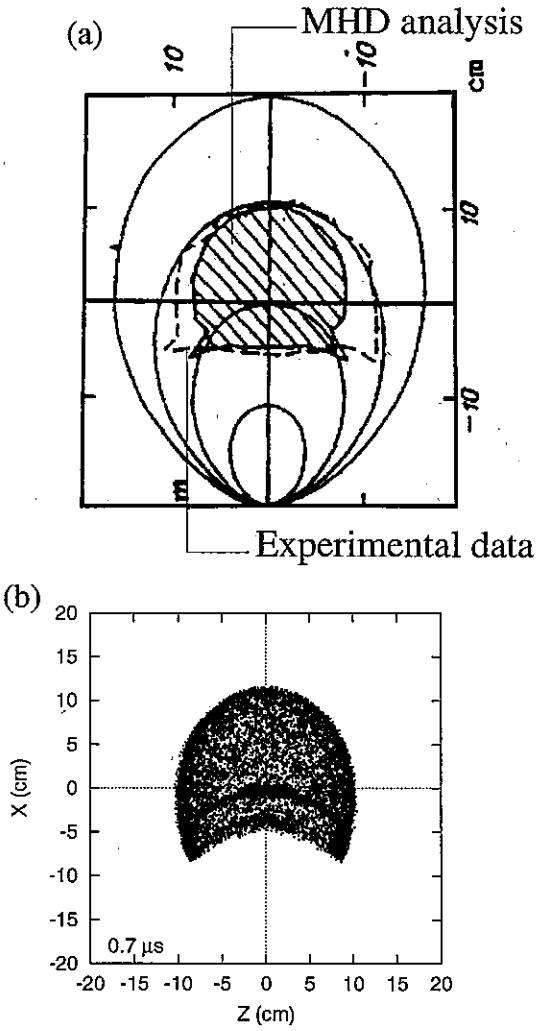

Fig. 9. (a) Experimental data (dashed line) and MHD calculational results (shaded area) of plasma cloud at time $t = 0.7\,\mu$s after laser pulse. (b) Simulation results of particle positions projected onto the xz plane at $t = 0.7\,\mu$s ($\kappa = 0.036$).

4.3 *"Rupture" mode analysis*

The "rupture" regime was studied by increasing the initial plasma energy and also the interaction parameter κ. We tried to simulate the case of $\kappa = 0.36$ with the initial plasma energy of 130 J. The maximum velocity of the plasma, V_m was 721 km/s. These values are one order of magnitude larger than those in the previous "quasi-capture" mode. (Note that the critical value for κ between the two modes is 0.1.)

Figure 13 shows the simulation result of particle positions projected onto the xz plane at time $= 0.3\,\mu$s after the laser pulse. Plasma particles are found to expand more rapidly at an early stage as compared with those in "quasi-capture" mode (Fig. 3). At $t = 0.32\,\mu$s, the plasma particles are found to move away from the calculation region and consequently we could not continue the calculation in the case of "rupture" mode, and the magnetic field could not capture the plasma cloud.

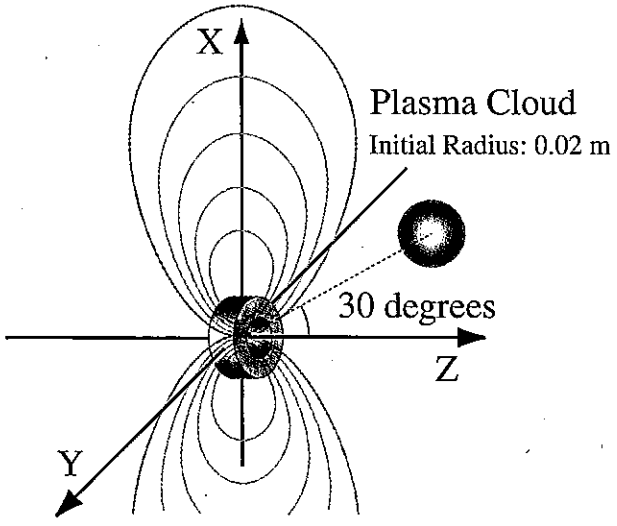

Fig. 10. Schematic of the calculation model.

5. Conclusion

We carried out analyses on plasma behaviors in a dipole field using a 3D hybrid code, and a comparison was made among the experimental data, MHD analysis and the results from the 3D hybrid code.

A parameter (interaction parameter) κ is defined, which characterizes the interaction between the expanding plasma and the dipole field.[1] The parameter has a critical value of 0.1. In the case where κ is less than 0.1, a substantial plasma deceleration will occur in all directions from the explosion lo-

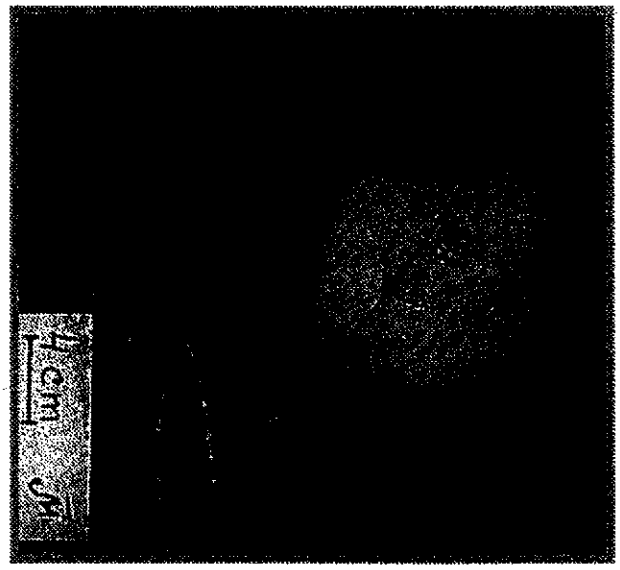

Fig. 11. Experimental data of plasma cloud at time $t = 0.55\ \mu s$ after laser pulse on xz plane ($\kappa = 0.02$).

cation (designated as "quasi-capture" mode). The plasma will not be captured by an ambient field when κ is greater than 0.1 (as "rupture" mode).

First, we analyzed the plasma in the case of "quasi-capture" mode with the parameters $\kappa = 0.02$ and 0.03. The initial plasma was located on the equatorial plane. Our numerical results on time evolution of particle position, particle velocity and magnetic field strength were presented. Comparison of the numerical results obtained by the 3D hybrid code with the MHD analysis and the experimental results, showed good agreement with regard to the motion of the plasma cloud and its macroscopic shape. The plasma cloud was captured in the dipole field and followed the field line, but it had a remarkable asymmetrical shape in the cross-field direction. This was due to the asymmetry of the diamagnetic motion and external magnetic field pressure on the right and the left sides of the plasma cloud. The formation of a diamagnetic cavity was also observed.

Second, the angular dependence of plasma expansion was discussed in the case of "quasi-capture" mode using the parameter $\kappa = 0.02$. The initial plasma was located 30 degrees from the z-axis. It is found that the plasma cloud expands under the ambient field configuration and its center moves away at an almost constant speed from the magnetic coil. In this case, the plasma cloud was not captured although the parameter κ was much lower than unity. This result is also in good agreement with the experimental one.

Finally, the "rupture" regime was studied by increasing the initial plasma energy and also the interaction parameter κ. We tried to simulate the case of $\kappa = 0.36$. The values are one order of magnitude larger than those of the previous "quasi-capture" mode. In this case, the plasma expanded rapidly and did not tend to be captured by an external field.

From these analyses, we found that the interaction parameter well characterizes the expansion behavior of the plasma in a dipole field if the plasma is located on the equatorial plane. If not, it would not be sufficient to characterize the plasma behavior only using the interaction parameter κ.

For future engineering applications, these results will be useful in designing an optimal configuration of the magnetic thrust chamber for laser fusion rockets, since the magnetic field structure adopted there is a variant of a dipole-type field.

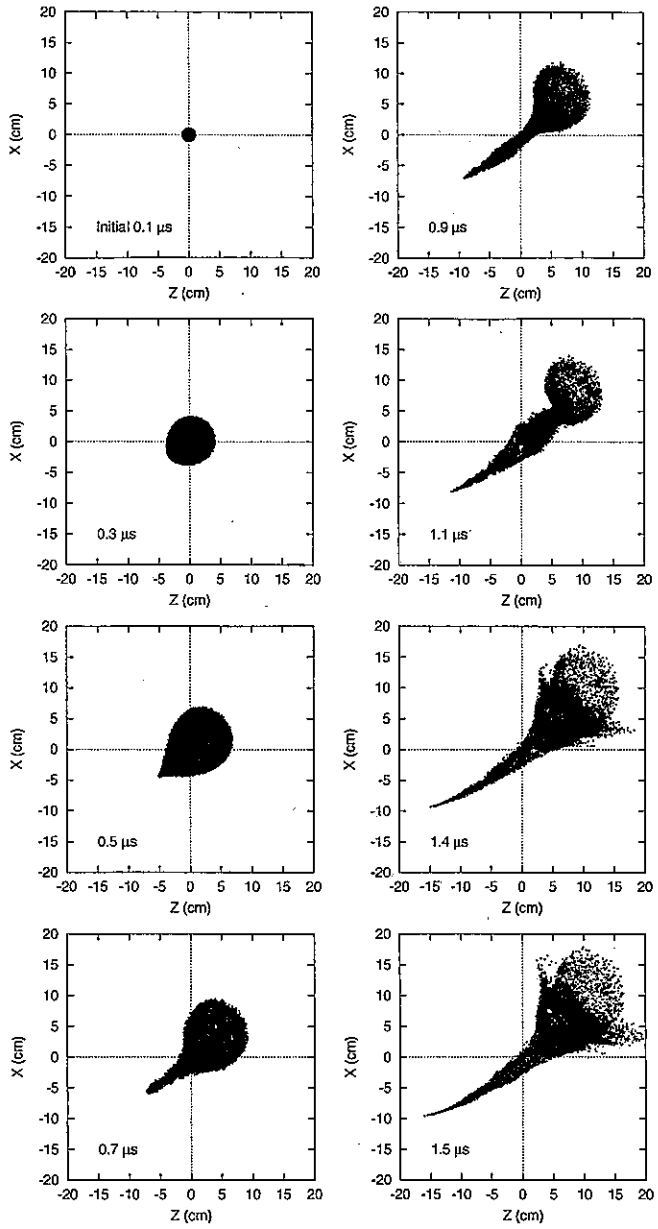

Fig. 12. Simulation results of particle positions from 0.1 μs to 1.3 μs projected onto xz plane ($\kappa = 0.036$).

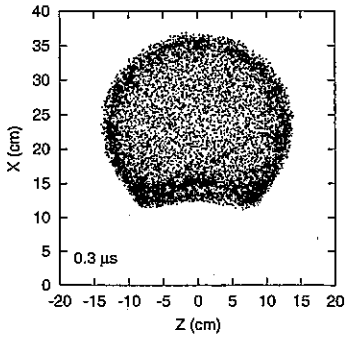

Fig. 13. Simulation results of particle positions projected onto the xz plane at $t = 0.3\ \mu s$ ($\kappa = 0.36$).

For the space plasma field, for instance, as the earth's magnetosphere is a dipole field, the effectiveness of methods for its protection from collisions with asteroids or comets should be studied.

Acknowledgements

This work is partly supported by the cooperative program of the National Institute for Fusion Science, and the numerical calculations were performed using the SX-4 at the institute.

1) S. A. Nikitin and A. G. Ponomarenko: J. Appl. Mech. & Tech. Phys. **34** (1993) 745.
2) Y. P. Zakharov, A. M. Orishich and A. G. Ponomarenko: Abstr. Conf. Hazard due to Comets and Asteroids, Tucsuon, USA, 1993, p. 88.
3) Y. P. Zakharov, A. G. Ponomarenko, H. Nakashima, T. Muranaka, H. Usui, S. A. Nikitin, J. Wolowski and E. Woryna: J. Plasma & Fusion Res. Ser. **2** (1999) 398.
4) Y. Nagamine and H. Nakashima: Fusion Technol. **35** (1999) 62.
5) H. Nakashima, Y. Nagamine, N. Yoshimi, Y. P. Zakharov and A. G. Ponomarenko: Fusion Eng. & Design **15** (1999) 255.
6) S. A. Nikitin and A. G. Ponomarenko: *Proc. Int. Conf. Emerging Nuclear Energy Systems, Herzliya, 1998* (Dan Knassim, Ramat Gan, 1998) Vol. 1, p. 299.
7) D. S. Harned: J. Comput. Phys. **47** (1982) 452.